The Impact of Detailed Snow Physics on the Simulation of Snow Cover and Subsurface Thermodynamics at Continental Scales

MARC STIEGLITZ

Lamont-Doherty Earth Observatory, Columbia University, Palisades, New York

AGNÈS DUCHARNE

UMR Sisyphe, Université Pierre et Marie Curie, Paris, France

RANDY KOSTER AND MAX SUAREZ

Hydrologic Sciences Branch, Laboratory for Hydrospheric Processes, NASA Goddard Space Flight Center, Greenbelt, Maryland

(Manuscript received 27 April 2000, in final form 6 December 2000)

ABSTRACT

The three-layer snow model of Lynch-Stieglitz is coupled to the global catchment-based land surface model of the National Aeronautics and Space Administration's Seasonal to Interannual Prediction Project, and the combined models are used to simulate the growth and ablation of snow cover over the North American continent for the period of 1987–88. The various snow processes included in the three-layer model, such as snow melting and refreezing, dynamic changes in snow density, and snow insulating properties, are shown (through a comparison with the corresponding simulation using a much simpler snow model) to lead to an improved simulation of ground thermodynamics on the continental scale. This comparison indicates that the three-layer model, originally developed and validated at small experimental catchments, does indeed capture the important snow processes that control the growth and the ablation of continental-scale snowpack and its snow insulation capabilities.

1. Background

Northern Hemisphere snow cover varies from 7% to 40% over the annual cycle, making it the most dynamic large-scale land surface feature on the earth (Hall 1988). As such, the large-scale spatial structure of snow cover can have an important impact on atmospheric circulation through its control over the land surface albedo and its impact on the surface energy balance (Barnett et al. 1989; Namias 1985). Historical data analysis has suggested that snow cover extent influences the development of the Asian monsoons in that an earlier snowmelt is associated with greater summer land heating and a stronger monsoon season (Dey and Bhanukumar 1983; Hahn and Shukla 1976; Kripalani et al. 1996; Ropelewski et al. 1984). More recently however, Kumar et al. (1999) have shown that the historical teleconnection between Eurasian snow cover and the Indian monsoon may have broken down under the influence of a long-term warming trend. Cohen and Entekhabi (1999) have suggested that anomalies in Eurasian snow cover lead to an expansion of the Siberian high over northern latitudes and, through a displacement of the Icelandic low, affect the North Atlantic oscillation. In turn, this results in colder surface air temperatures in eastern North America and western Europe as well as wetter conditions in southern Europe and the Mediterranean. Last, at the regional scale, snow heterogeneity within a landscape has been found to influence mesoscale wind patterns (Johnson et al. 1984; Segal et al. 1991). Hence, accurate long-term forecasts in a fully coupled climate system can be strongly dependent on an accurate simulation of the snow-covered area, snow water equivalent, and snow depth.

With respect to terrestrial hydrologic processes, snow cover plays an important role in springtime runoff generation and flood production. In many northern-latitude regions, as well as regions with high relief, spring meltwater derived from the winter snow pack represents the greatest source for the yearly ground moisture budget (Aguado 1985). Further, at high latitudes the magnitude and timing of spring snowmelt water delivered to the

Corresponding author address: Marc Stieglitz, Lamont-Doherty Earth Observatory, Route 9W, Palisades, NY 10964.
E-mail: marc@ldeo.columbia.edu

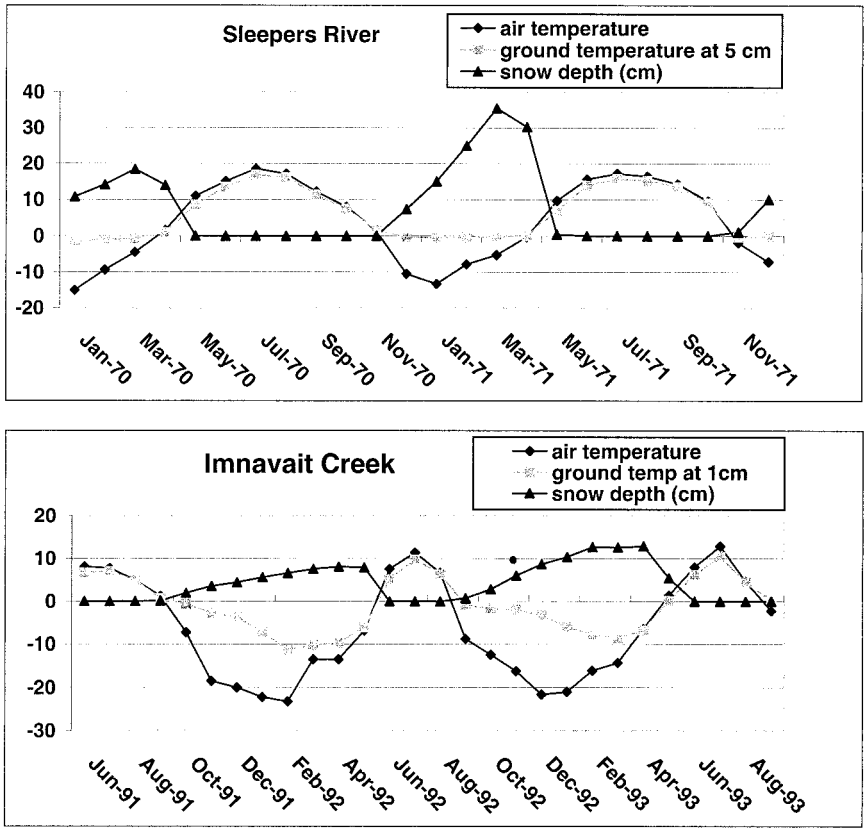

FIG. 1. Overlying air temperature, modeled surface ground temperature, and modeled water equivalent snow depth at two sites with significant snow cover: (top) the Sleepers River NOAA–ARS snow research station located in the highlands of east-central Vermont and (bottom) the Imnavait Creek watershed located in the foothills of the Brooks Range on the North Slope of Alaska. For both sites, model-generated data were in good agreement with the intermittently measured site validation data (Lynch-Stieglitz 1994; Stieglitz et al. 1999). Temperatures are in degrees Celsius.

Arctic Ocean affect the stability of the ocean's surface layer and thereby affect ocean circulation and seasonal sea ice formation (Mysak and Venegas 1998).

Because a snowpack is thermally insulating and limits the otherwise efficient heat exchange between the ground and the atmosphere, it controls the evolution of wintertime ground temperatures (Lynch-Stieglitz 1994). Through freeze–thaw activity, this control over the evolution of ground temperatures influences the downslope redistribution of shallow ground water, surface runoff, and evapotranspiration. Ground temperatures in turn also influence soil microbial activity and the associate fluxes of carbon dioxide (CO_2) and methane (CH_4) to the atmosphere (Billings et al. 1982; Walter et al. 1996). Both CO_2 flux tower measurements and modeling studies show that a longer growing season, associated with a shorter snow season, is positively correlated with a net annual carbon sequestration (Goulden et al. 1996, 1998; Stieglitz et al. 2000). Further, because of the greenhouse capacity of trace gases, the interaction between ground freezing, vegetation, and release of soil carbon as CO_2 or CH_4 can also lead to climate feedbacks that act on longer timescales (McFadden et al. 1998).

As a practical demonstration of the impact that snow insulation has on the evolution of ground temperatures, Fig. 1 shows air and ground temperatures at two sites for which seasonal snow cover is significant: Sleepers River, Vermont, and Imnavait Creek, Alaska. During the summer months, when the snowpack is nonexistent, the air and surface ground temperature track each other with only a small offset in temperature. However, once the snow begins to accumulate, the relatively warm ground is insulated from the cold atmosphere and ground temperatures remain warm throughout the season. In effect, the pack prevents the escaping of heat from the warm ground to the atmosphere, or conversely, damps out the cold wintertime temperature signal in the snowpack well before it reaches the ground.

Despite the acknowledged role that the snow cover plays in regulating the earth's global water and energy budgets, most land surface models (LSMs) intended for use in exploring the above-mentioned feedbacks (i.e.,

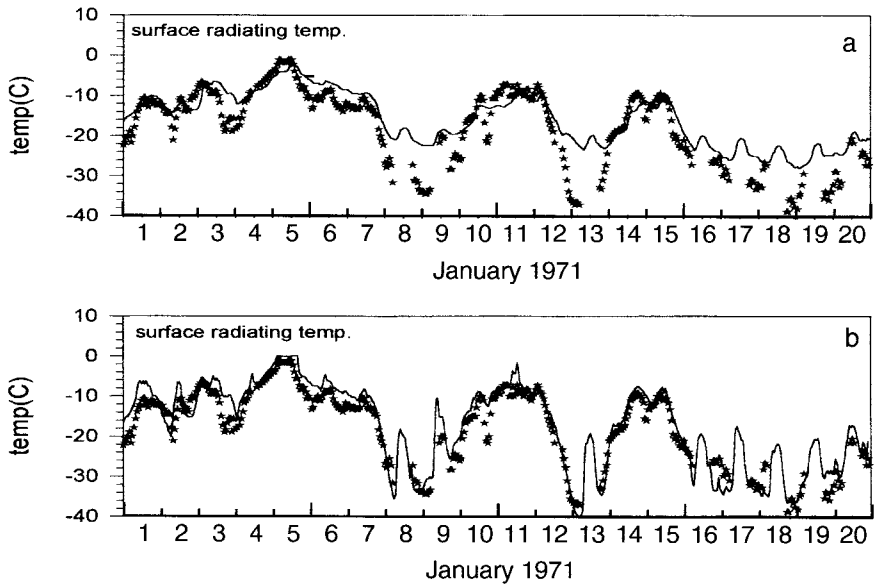

FIG. 2. (a) Measured hourly surface radiating temperature for 20 days starting 1 Jan 1971 at the NOAA–ARS research station (stars) and predicted by an LSM without snow insulation (solid line). (b) Measured hourly surface radiating temperature for 20 days starting 1 Jan 1971 at the NOAA–ARS research station (stars) and predicted by an LSM using the three-layer snow model of Lynch-Stieglitz (1994) (solid line).

coupled with atmospheric circulation models, ocean, and sea-ice models) are inadequate for modeling high-latitude processes. Previous work on the development of land surface schemes has primarily focused on developing multiple-layer soil column models and improving canopy processes, with little attention paid to high-latitude processes and, more specifically, snow physics or permafrost dynamics. As a step toward addressing this deficiency, the three-layer snow model of Lynch-Stieglitz (1994) has recently been coupled to the catchment-based LSM (Ducharne et al. 2000; Koster et al. 2000a) that is currently being developed under the auspices of the National Aeronautics and Space Administration's (NASA) Seasonal to Interannual Prediction Project (NSIPP) [see section 2a(2)]. We demonstrate in this paper that through a sufficient representation of snow processes, we significantly improve the LSM's simulation of high-latitude processes, particularly the evolution of subsurface ground temperatures.

2. Modeling snow cover

Although sophisticated multilayer snow models have been developed and successfully applied at the local scale (Anderson 1976; Brun et al. 1989; Hardy et al. 1998; Jordan et al. 1999; Lynch-Stieglitz 1994), the treatment of snow processes, especially those used within general circulation models (GCMs), have been relatively simple. Some models consider the winter snow pack only as a store of moisture (Abramopoulos et al. 1988; Bonan 1996; Koster and Suarez 1996), and others blur the distinction between the snow and the ground surface altogether by envisioning a composite soil and snow layer (Dickinson et al. 1993; Pitman et al. 1991). Still others do distinguish between separate snow and ground layers yet represent the entire pack with a single snow layer regardless of the actual pack depth (Slater et al. 1998; Verseghy 1991).

Simulations at the National Oceanic and Atmospheric Administration–Agricultural Research Service (NOAA–ARS) snow research station, located within the Sleepers River catchment of northern Vermont, demonstrate how such simple representations of snow and cold season processes can lead to a corruption of surface energy fluxes and a degradation of the snow insulation between the cold atmosphere and the warm ground (Lynch-Stieglitz 1994). Hourly hydrometeorological data were used to force an LSM (Abramopoulos et al. 1988) that treated snow cover as nothing more than a store of water and energy; that is, the snowpack offered no insulation to the underlying ground. Without this insulation effect, there is nothing to prevent the escaping of heat from the warm ground to the cold atmosphere. As such, the large wintertime thermal gradient that exists between the cold atmosphere and warm soils results in an upward transfer of heat within the soil column. This heat is then imparted to the snowpack, which in turn radiates the energy out to space. The unrealistically warm modeled surface snow radiation temperatures shown in Fig. 2a reflect this steady supply of heat that is being imparted to the snowpack. Note that periods when the air temperatures drop most dramatically are associated with the largest air–soil temperature gradient, the largest upward soil heat flux, and the largest over-

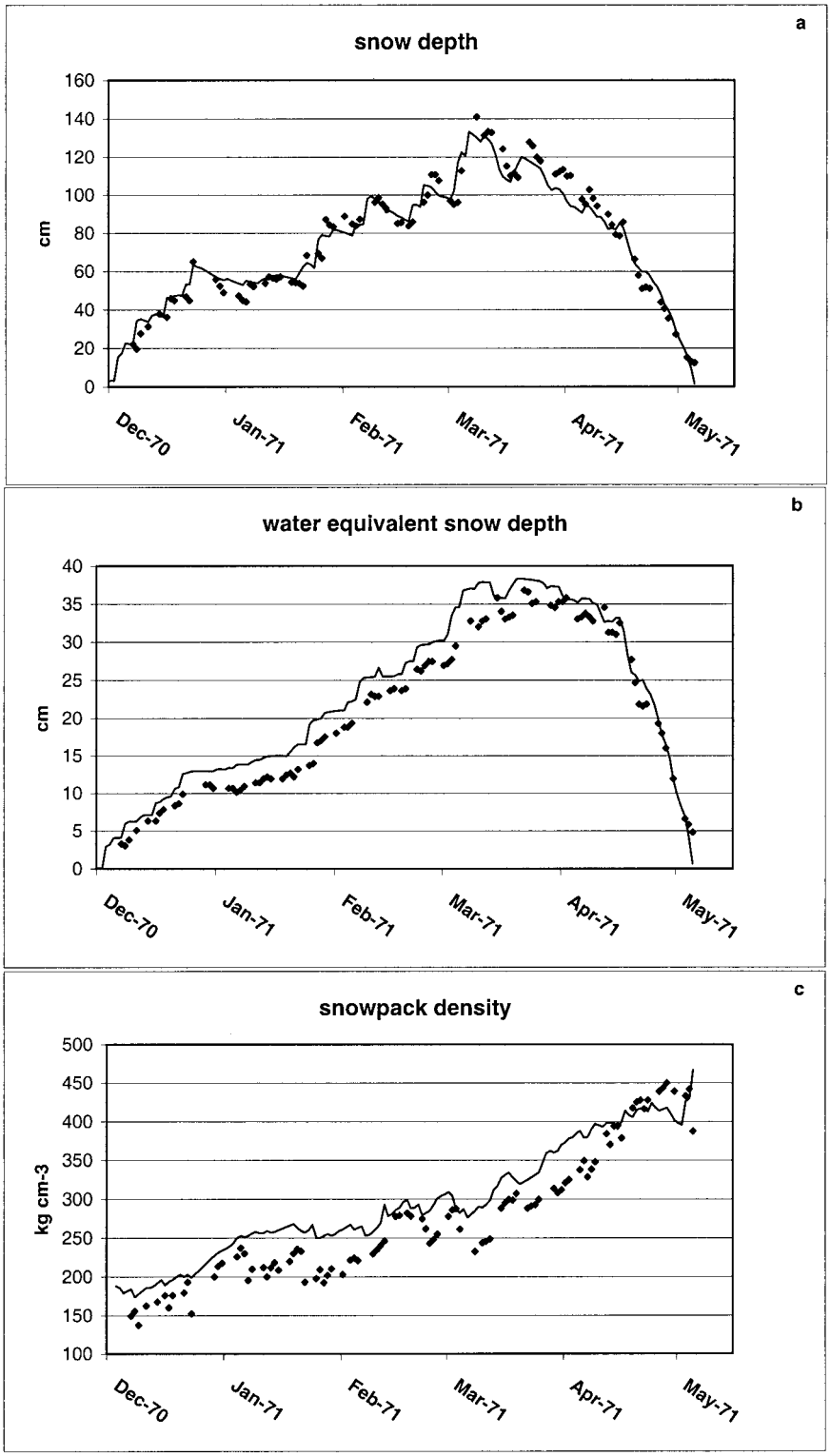

FIG. 3. (a) Snow depth, (b) water equivalent snow depth, and (c) snowpack density for 1970–71 measured at the NOAA–ARS research station (diamonds) and predicted by an LSM with the three-layer snow model of Lynch-Stieglitz (1994) (solid line).

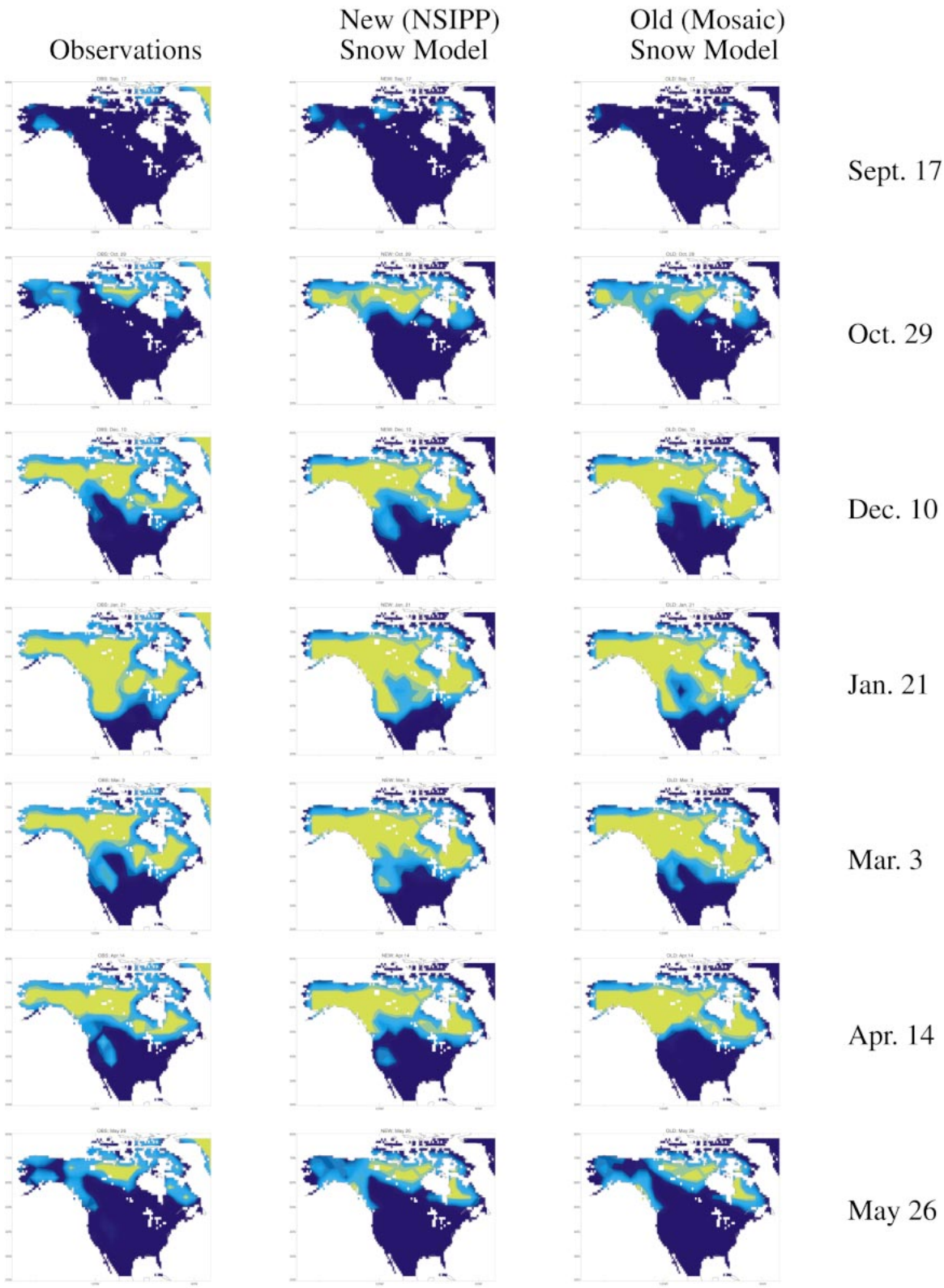

FIG. 4. Measured and modeled spatial evolution of fractional snow coverage over the approximately 5000 catchments composing North America for the 1987/88 snow season (blue = 0, green = 1).

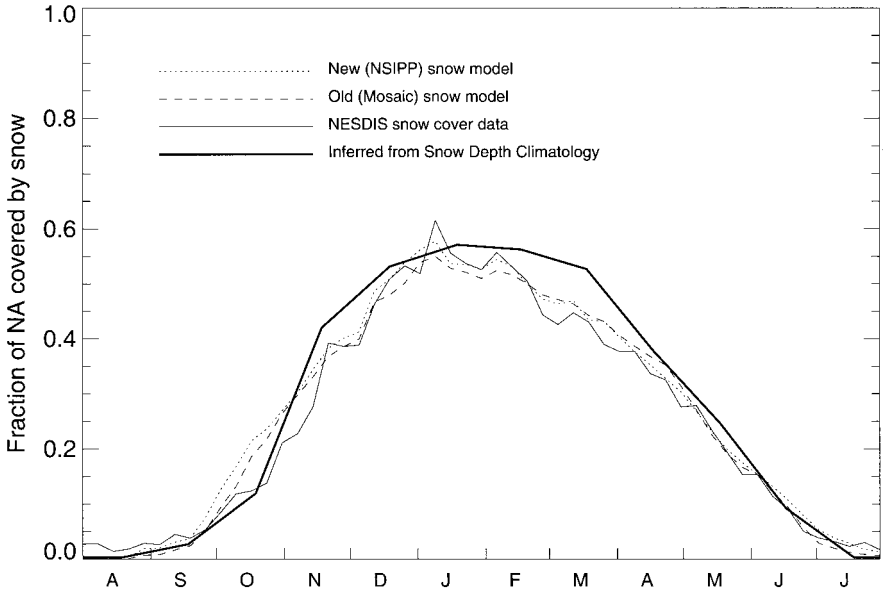

FIG. 5. Fractional snow coverage over North America for the period of 1 Aug 1987 through 31 Jul 1988 for both the old Mosaic and new NSIPP snow scheme as well as coverage determined from satellite [NOAA/National Environmental Satellite, Data, and Information Service weekly snow coverage, found on the ISLSCP CD-ROM or the Lamont-Doherty Earth Observatory climate data library (LDEO 2000)] and from ground stations [Environmental Technical Applications Center (ETAC) Air Force climatological dataset; Foster and Davy 1988].

estimation of snow surface temperatures. This transfer of heat from the soil column to the atmosphere leads to unrealistic cooling and freezing of the soils. Further, this freezing (to a depth of 2 m) represents such a large heat loss from the ground system that deeper layers do not unfreeze until late summer, obviously affecting the normal seasonal evolution of hydrologic processes such as runoff, ground water movement, infiltration, and evapotranspiration.

Recently, sophisticated snow physics have been included in some LSMs and demonstrate a clear improvement in the overall simulation of the hydrologic cycle at the catchment scale (Loth and Graf 1998a,b; Loth et al. 1993; Lynch-Stieglitz 1994; Stieglitz et al. 1997; Yang et al. 1997). We now present the coupling of the Lynch-Stieglitz (1994) snow model to the NSIPP catchment-based LSM (hereinafter referred to as the NSIPP snow model). Validation for the 1987/88 snow season over North America is also presented. Via comparisons with corresponding simulations that use the much simpler ''Mosaic'' snow scheme (Koster and Suarez 1996) coupled to the NSIPP LSM (hereinafter referred to as the Mosaic snow model), we will demonstrate that the more sophisticated model can overcome the deficiencies outlined above at the continental scale.

a. The NSIPP snow model: Coupling a three-layer snow model to the NSIPP catchment-based LSM

1) A THREE-LAYER SNOW MODEL

This three-layer snow model accounts for snow melting and refreezing, dynamic changes in snow density, snow insulating properties, and other physics relevant to the growth and ablation of the snowpack. The upper boundary of the snowpack moves up and down under the influence of snowfall, mechanical and wet compaction, condensation, and sublimation. We now discuss these processes in turn.

The snowpack is modeled with three snow layers. Three variables are used to describe the system: layer thickness (Z_i), water equivalent (W_i), and heat content (H_i). Heat and mass (water) flow within the pack are explicitly modeled. Radiation conditions, as well as the evolution of the snow albedo, determine the surface energy fluxes. Heat flow within the pack is accomplished solely via linear diffusion along the thermal gradient. A volumetric water holding capacity characterizes each snow layer. As such, meltwater generated in a layer will remain in the layer if the liquid water content of the layer is less than the layer holding capacity. Otherwise, it will flow down to a lower layer where it will refreeze in the layer, remain in the layer in the liquid state, or pass through. Two independent processes govern densification of the pack. A simple parameterization is used to describe mechanical compaction, or compaction due to the weight of the overburden (Kojima 1967; Pitman et al. 1991), and a separate densification is accomplished via the melting–refreezing process. Snowfall, rain, evaporation, sublimation, and condensation represent sources and sinks of mass and heat into the uppermost snow layer. Last, resolution requirements dictate that to capture reasonably the diurnal range in the surface radiation temperature the upper surface layer

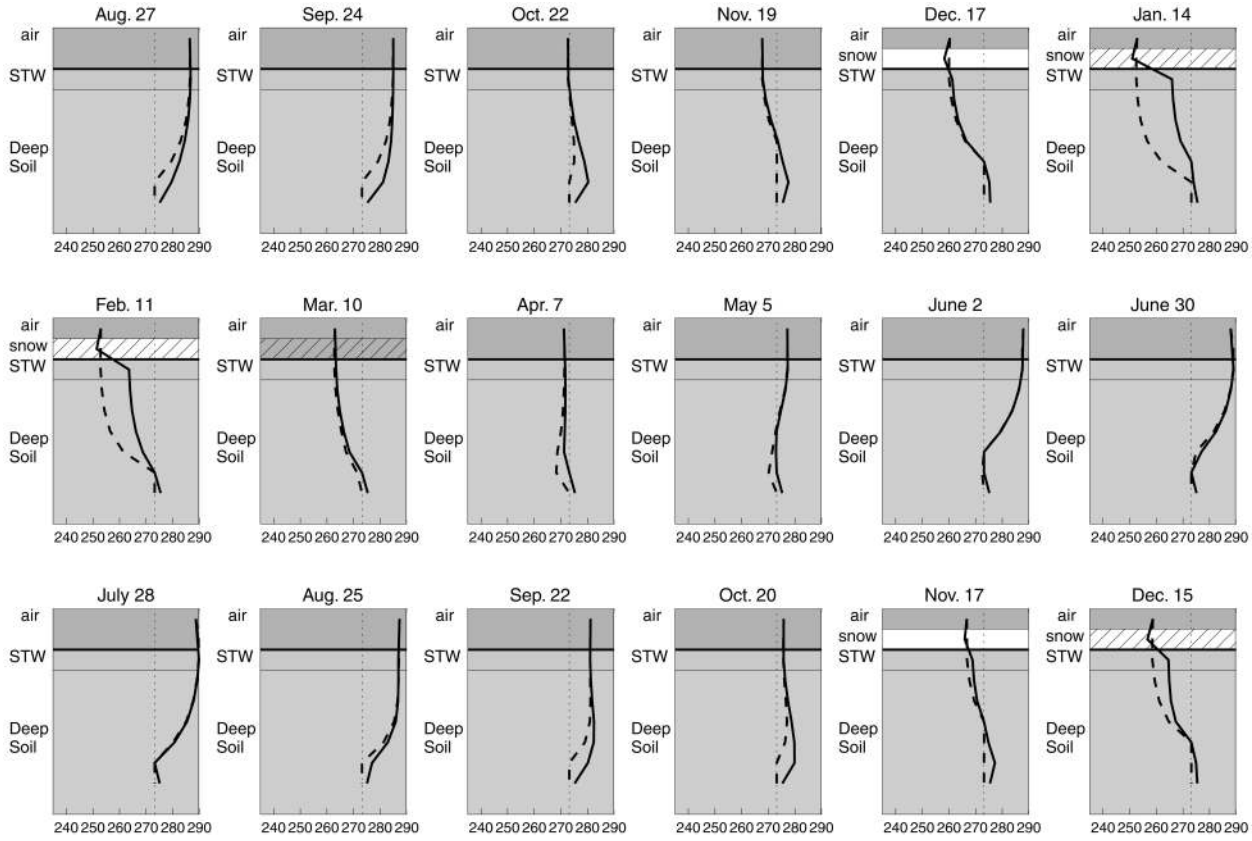

FIG. 6. The evolution of ground temperatures at depth for the 1987/88 snow season at 54°N, 99°W. The presence or absence of snow in the new NSIPP model is indicated by the white region labeled ''snow.'' The presence or absence of snow in the old Mosaic model is indicated by the stippled region. A layer that is both white and stippled indicates the presence of snow cover in both the new and old snow models. STW refers to the uppermost soil layer. Temperature profiles using the new NSIPP snow model are shown with a solid line. Temperature profiles using the old Mosaic snow model are shown with a dashed line. Ground temperatures are in kelvins.

can be no greater than the thermal damping depth of snow, approximately 6–10 cm. This requires that at every time step a simple masswise redistribution of heat and water contents are performed among the three model layers.

Results at the Sleepers River snow research station demonstrate the superiority of using this three-layer model instead of the simpler Abramopoulos et al. (1988) snow scheme discussed above. Not only are the radiation temperatures of the ground and snow surface now adequately modeled (Fig. 2b), but all the features of snowpack ripening that characterize pack growth/ablation are also well simulated (Fig. 3) (Lynch-Stieglitz 1994).

2) THE NSIPP CATCHMENT-BASED LSM

The catchment-based LSM was developed to overcome a critical deficiency in standard GCM-based LSMs, namely, the neglect of an explicit treatment for spatial variability in soil moisture. Standard LSMs employ a one-dimensional treatment of subsurface moisture transport and surface moisture and energy fluxes that effectively assumes homogeneous soil moisture conditions across areas spanning hundreds of kilometers. Much recent development work by various groups has focused on improving the 1D representation itself, incorporating, for example, more physiologically based vegetation schemes so as to determine transpiration and canopy–atmosphere CO_2 fluxes better (Bonan 1995; Kucharik et al. 2000; Sellers et al. 1986). Relatively little attention has been given to the spatial heterogeneity issue, which is unfortunate given that this heterogeneity can have a strong impact on surface energy and water budgets.

The strategy (Koster et al. 2000a) calls for the partitioning of the continental surface into a mosaic of hydrologic catchments, delineated through analysis of surface elevation data. Thus, the effective ''grid'' used for the land surface is not specified by the overlying atmospheric grid. Within each catchment, the soil moisture variability is related to characteristics of the topography and to three bulk soil moisture variables through a ''TOPMODEL''-type formulation of catch-

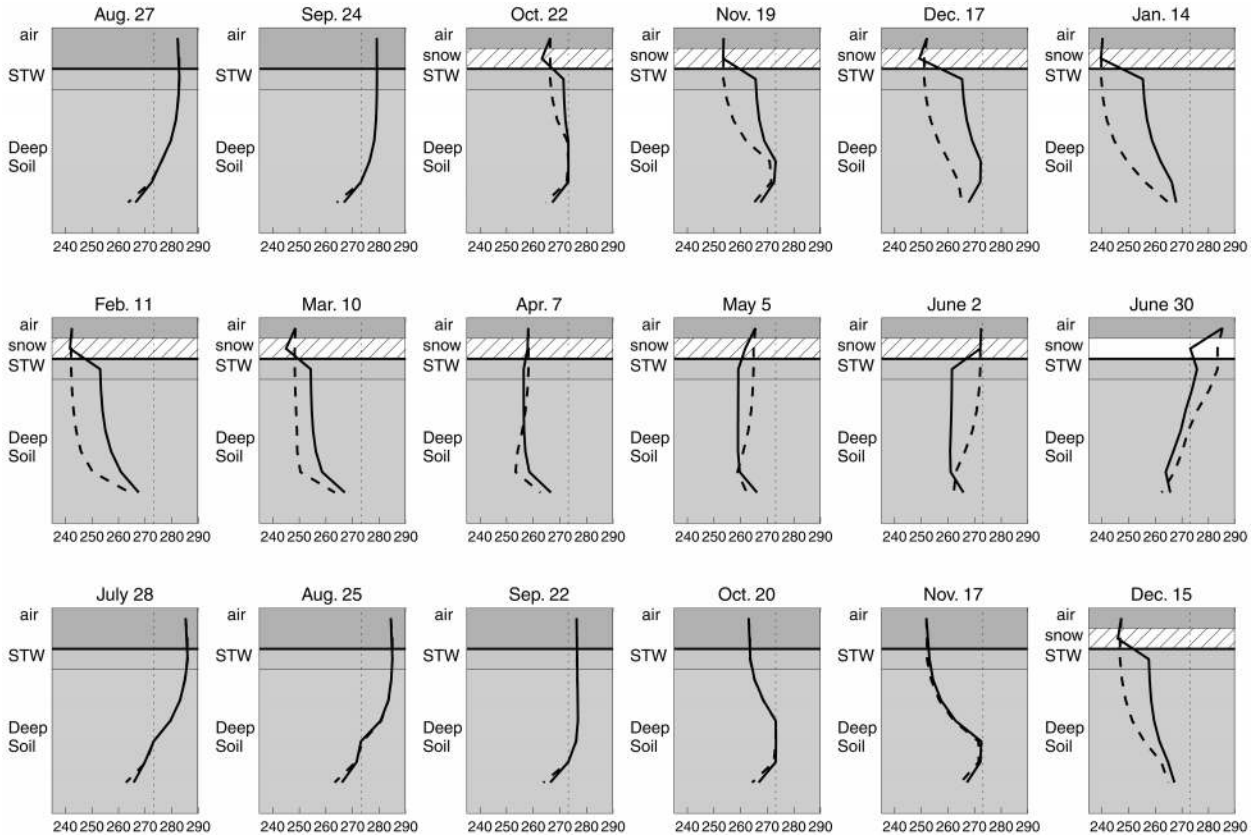

FIG. 7. As in Fig. 6, but at 61°N, 99°W.

ment processes (Beven and Kirkby 1979). Many of the ideas underlying the strategy are culled from the works of Beven and Kirkby (1979), Famiglietti and Wood (1991), Sivapalan et al. (1987), and Stieglitz et al. (1997), among others.

A particularly unique aspect of the NSIPP catchment model is the separation of the catchment into three subregions, each representing a distinct hydrological regime: one in which the surface is saturated, one in which the surface is unsaturated but transpiration proceeds without water stress, and one in which transpiration is stressed. Because these subregions are tied to the dynamically varying moisture variables in the catchment, their sizes vary with time. Key to the modeling strategy is the application of different formulations of evapotranspiration and runoff in each subregion to reflect the fundamentally different physical mechanisms controlling these fluxes in the three regions. This is a far more physically consistent approach than is possible with traditional one-dimensional LSMs.

Transpiration and other surface energy balance calculations proceed using established and tested code from a standard soil–vegetation–atmosphere (SVAT) transfer–type vegetation model (Koster and Suarez 1992a, 1996) that includes bare soil evaporation and canopy interception loss. The SVAT code used for one-dimensional energy balance calculations is applied over each of the three identified moisture regimes. Each moisture subregion maintains its own prognostic surface temperature; no ''smoothing out'' of this temperature is performed at the end of a time step. This allows the valley bottoms, where more evapotranspiration occurs, to remain consistently cooler than the drier uplands.

Of particular relevance here is the treatment of ground thermodynamics. Although each of the three subregions maintains its own surface/canopy temperature, temperatures for deep soil levels are assumed to be spatially homogeneous. The net heat flux from model surface soil layer to the layer just below is computed by weighting the individual heat flux from each moisture subregion by its respective area and then summing together the three weighted fluxes. The top layer's thickness is taken to be 5 cm to allow us to capture the diurnal range in the surface radiation temperature. To be compatible with the assumption that a zero heat flux condition applies at the bottom boundary of the deepest model layer, the ground profile extends to a depth of 10 m, approximately three times the seasonal damping depth for typical soils.

The NSIPP model has been tested offline over the Red River–Arkansas River basin, using forcing established for the Project for Intercomparison of Land Surface Parameterization Schemes 2c intercomparison

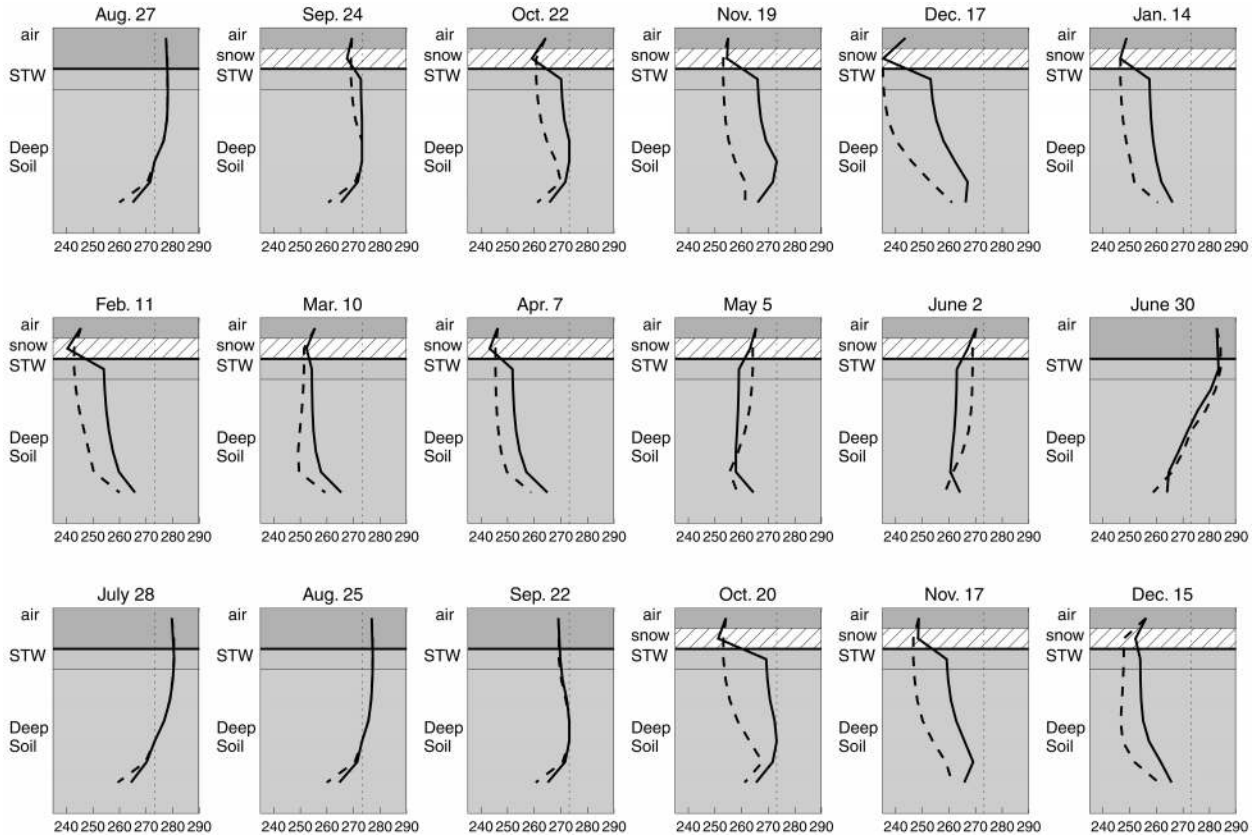

FIG. 8. As in Fig. 6, but at 68°N, 159°W.

study (Wood et al. 1998). With a minimal amount of calibration, the catchment model reproduces the observed surface fluxes in the basin and the interannual variability with high accuracy (Ducharne et al. 2000).

3) COUPLING THE SNOW MODEL TO THE CATCHMENT-BASED LSM

Coupling the three-layer snow model to the catchment framework necessitated some modifications to the above described 1D snow scheme. In particular, we now ensure a smooth transition between snow-free and snow-covered conditions to capture the gradual growth and ablation of a snowpack's spatial extent and to avoid abrupt (discontinuous) changes in the surface energy balance calculations. The approach used is straightforward. We assume a minimum local snow water equivalent SWE_{min} of 13 mm. If a given volume of snow falls on a snow-free catchment, that volume is spread uniformly over a fraction of the catchment so that the local water equivalent at any snow-covered point is SWE_{min}. Thus, if the snow falling on a snow-free catchment during a time step has a total water equivalent volume V_s and if the area of the catchment is A, then the snow-covered area A_s is taken to be $V/(SWE_{min})$. The snow-covered areal fraction A_s/A increases as more snow falls until it reaches 1, at which time the local snow water equivalents across the catchment start increasing uniformly. When the fractional coverage is less than 1, the snow model is represented with a single snow layer, whereas three model layers are used when the snow coverage is complete (Lynch-Stieglitz 1994). The transition between the single-layer and three-layer representations involves a simple conservative redistribution of layer heat and water contents. Surface energy calculations are performed separately over the snow-free and snow-covered areas. With 13 mm as the value for SWE_{min} we can both resolve the diurnal surface temperature signal and at the same time produce a stable solution with a 20-min GCM time step.

Each catchment is assigned a single vegetation or bare soil type (Koster and Suarez 1992b, 1996) As such, the catchment-wide albedo is determined from the current snow amount and the snow masking depth that is associated with each vegetation type (Hansen et al. 1983). In the presence of snow, it is presumed that a fraction of the green vegetation is masked by snow. The resulting catchment albedo is therefore a weighted composite of the albedo for the green fraction and the snowpack albedo for the masked fraction. For computational simplicity we appropriately modify the snowpack albedo formulation of Hansen et al. (1983), in which albedo is

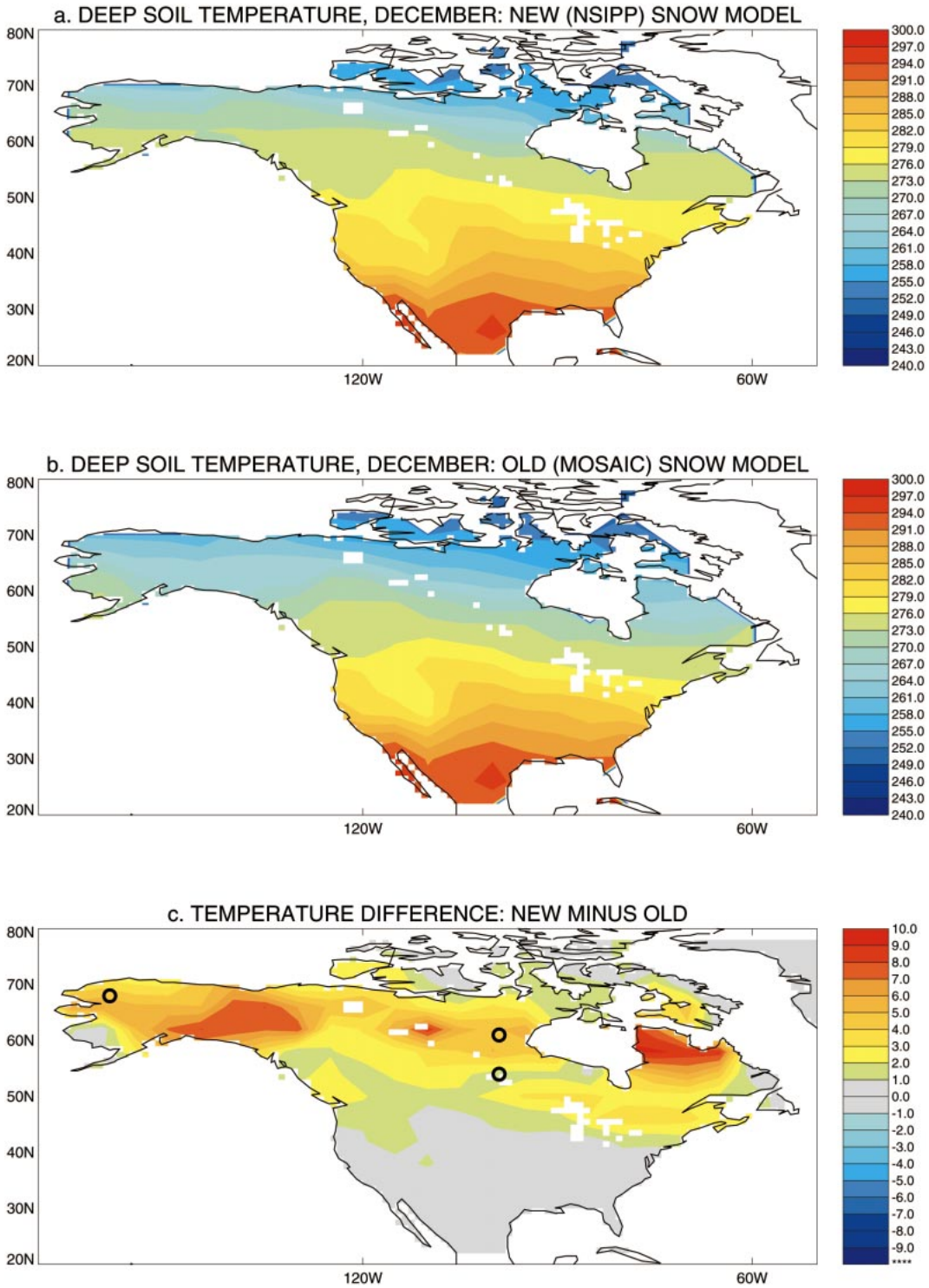

FIG. 9. (a) Deepest soil layer temperatures for the NSIPP snow model after the 10-yr spinup. (b) Deepest soil layer temperatures for the Mosaic snow scheme after the 10-yr spinup. (c) The spatial difference in temperatures for the deepest soil layer between the new NSIPP snow model and old Mosaic snow scheme after the 10-yr spinup. In Figs. 6–8, the seasonal evolution of ground temperatures was presented (at 54°N, 99°W; 61°N, 99°W; and 68°N, 159°W). The small circles in (c) correspond to these locations.

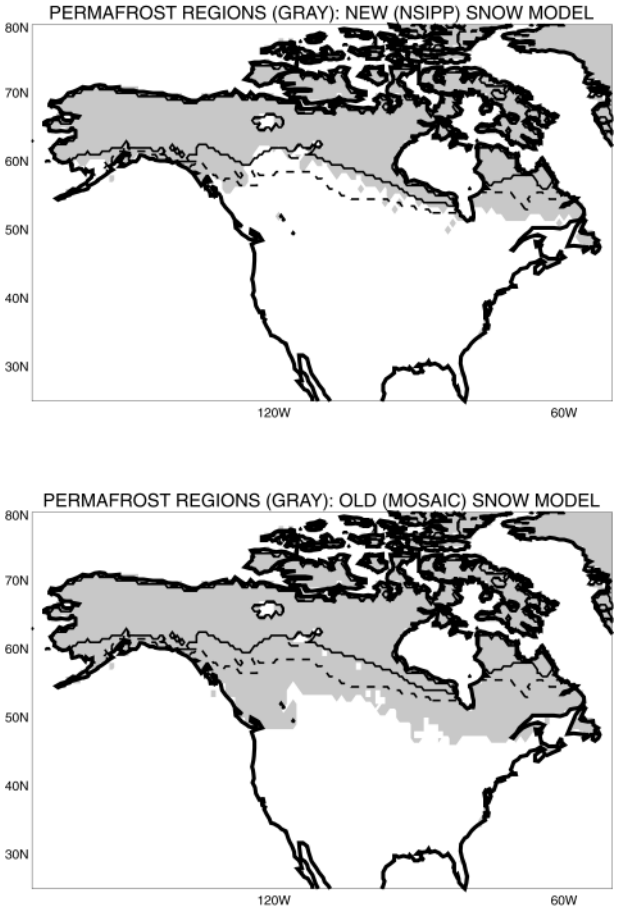

FIG. 10. Model-generated and observed (NSIDC digital permafrost maps; Zhang et al. 1999) permafrost regions. A catchment is considered to be within a permafrost region and thereby shaded gray if the deepest model layer within that catchment is frozen throughout the 1987–88 simulation period. The solid line refers to the observed permafrost line corresponding to 50% permafrost coverage, whereas the dashed line corresponds to 10% permafrost coverage. With few exceptions, the permafrost boundary generated by the new scheme is highly accurate.

parameterized as a function of snow surface aging, to instead be a function of the density of the snow surface layer.

b. The Mosaic snow model: A simpler scheme

One of the goals of this paper is to demonstrate that the physics incorporated into the three-layer snow model leads to an improved simulation of snow processes at the continental scale. We thus examine the behavior of a less sophisticated model in conjunction with that of the new NSIPP snow model.

The less sophisticated model chosen for the comparison is the snow module of the Mosaic land surface scheme (Koster and Suarez 1996). This model tracks the growth and ablation of snow using a single moisture reservoir. Compaction, liquid water storage, refreezing, and other such processes within the snowpack are ignored; nevertheless, conservation of snow water is strictly maintained. The entire snowpack is assumed to have the same temperature as the underlying surface soil, and a single energy balance is calculated for the combined snow–surface soil system. Snow, of course, affects this calculation by imposing its own albedo (which accounts for subgrid snow coverage but not for snow aging) and by providing an energy sink during snowmelt.

The Mosaic land surface scheme has been used in numerous GCM studies (Koster and Suarez 1995; Koster et al. 2000b), and its snow module has proven to be robust. Foster et al. (1996) present a comparison of observed continental-scale snow cover with the snow cover generated by several GCMs, including the GCM coupled to the Mosaic scheme. Although the Mosaic snow scheme produced a reasonable simulation of snow cover in that study, it tended to underestimate snow water equivalent. Model errors identified in the Foster et al. (1996) study, however, also reflect errors in the GCM's simulated precipitation and temperature forcing.

3. Validation over North America

At the continental scale we can evaluate the ability of the new NSIPP snow model to simulate spatial coverage of snow, as well as snow amounts, over large areas. To this end, the International Satellite Land Surface Climatology Project (ISLSCP) Initiative-1 CD-ROM (Sellers et al. 1996) data were used to drive the model over North America for the 2-yr period of 1987–88. The Northern Hemisphere Equal-Area Special Sensor Microwave Imager Earth Grid (EASE-Grid) Weekly Snow Cover dataset is used to evaluate simulated snow coverage (NSIDC 1996). Further, using the National Snow and Ice Data Center (NSIDC) digital permafrost maps (Zhang et al. 1999) we can evaluate the impact that snow insulation has on the evolution of ground temperatures, specifically, the evolution of the southerly extent of the continental permafrost front.

For the current analysis, the coupled NSIPP catchment/snow model was driven over North America [partitioned into about 5000 catchments based on the U.S. Geological Survey's Earth Resources Observation Systems Data Center's ''GTOPO30'' global 30–arc second elevation data (Verdin and Verdin 1999)], using hourly atmospheric forcing derived from the ISLSCP Initiative-1 CD-ROM (Sellers et al. 1996). Based on vegetation maps, each of the 5000 catchments were assigned to be either one of six vegetation types or bare soil (Koster and Suarez 1996). Spinup of model variables was achieved by cycling the model through the two years of forcing data at least five times, with model diagnostics saved only during the final cycle.

The same spinup process was then repeated using the NSIPP catchment-based LSM coupled to the Mosaic snow model (see section 3b above). For logistical rea-

sons, the version of the catchment model used here was older and somewhat inferior to that which was used with the three-layer snow scheme, with differences mainly in the representation of soil/catchment hydrologic representations. However, because the current analysis focuses on snow dynamics and subsurface thermodynamics and because both versions of the catchment model employed the same subsurface heat diffusion algorithm, the comparison should be valid. In essence, the differences induced by using two different versions of the catchment model are confined to snow-free periods.

Figures 4 and 5 show the spatial evolution of snow coverage over North America for the 1987/88 snow season. Both the Mosaic snow model and the NSIPP snow model capture this evolution fairly well. Considering that the major drivers for both schemes are the total atmospheric radiation, air temperature, and precipitation, this result is somewhat expected. When atmospheric conditions favor snowfall, snow cover accumulates, and when conditions shift in favor of melting, the pack ablates. The ground–snow heat flux has significantly less impact on pack growth and ablation than does the atmosphere–snow flux. However, as demonstrated in Lynch-Stieglitz (1994), this does not imply that the surface radiation temperatures evolve similarly with both models. Therefore, when the land–atmosphere feedbacks are possible (i.e., in coupled land–atmosphere runs), the spatial evolution of the snowpack may evolve differently for the two schemes over the course of a snow season.

To understand better the control that snow insulation has over the evolution of the ground thermal processes, Figs. 6–8 show ground temperatures with depth at three locations (54°N, 99°W; 61°N, 99°W; 68°N, 159°W) for the 1987/88 snow season. The length of the snow season increases from 4 months at 54°N to just less than 10 months at 68°N. In all cases, the impact of snow insulation is clear. In the Mosaic snow model, the ground and atmosphere are effectively in direct contact regardless of the intervening snowpack, and with the onset of winter the soil is quickly depleted of heat content. With the new NSIPP snow scheme, on the other hand, the ground heat reservoir, which has been gaining energy throughout the warm summer months, is effectively cut off from the cold atmosphere once snow cover accumulates, and this cutoff minimizes heat loss. A comparison of model-generated results at 61°N with data taken at the nearby Boreal Ecosystem–Atmosphere Study sites (Levine and Knox 1997; Pauwels and Wood 1999) demonstrates that midwinter temperatures in the old scheme are too cold by approximately 15°–20°C, but the new scheme evolves ground temperatures in close agreement to site data. Note, however, that, except for differences in the deep model temperatures, the profiles are remarkably similar by the end of the summer; that is, the soil heat memory is only on the order of several months. In any case, the impact of extreme ground freezing with depth in the midwinter using the old scheme can have profound implications for both hydrologic and biologic processes, as well as for the proper simulation of the surface energy fluxes. For example, the extremely cold midwinter ground temperatures will effectively shut off microbial respiration, which has been shown to operate at temperatures as low as −7°C. As demonstrated by Oechel and others (Oechel et al. 1997; Zimov et al. 1993, 1996), this winter respiration can account for as much as 30% of the annual soil respiration at high latitudes.

Figure 9 shows that the spatial differences in temperatures for the deepest soil layer between the new NSIPP and old Mosaic snow scheme after the models have been spun up can be as much as 9°C. The reason for this difference is as follows. As snow accumulates, the ground under the new NSIPP snow model is insulated from the cold winter air temperatures and, as a result, evolves a deep ground temperature that is considerably higher than the overlying mean annual air temperature. On the other hand, the old Mosaic scheme, which has no representation of snow insulation, continually loses heat to the atmosphere until equilibrium is reached, at which point the deep ground temperature is close to the long-term air temperature overlying a given region. Further, the general trend is such that the deep soil temperature difference between the models increases with latitude, corresponding to a longer snow season with latitude and therefore a longer period in which winter snow insulation is operating in the new model. For similar reasons, regions showing an especially large difference, east of Hudson's Bay and north of the Gulf of Alaska, are regions where the new NSIPP snow scheme predicts earlier snow accumulation and later melt than the old Mosaic snow scheme does (see Fig. 4).

The fact that the soil heat content using the old Mosaic snow scheme is less than that of the new NSIPP snow scheme, especially at lower latitudes, is reflected in the permafrost maps in Fig. 10. Here we consider a catchment to be within a permafrost region and thereby shaded gray if the deepest model layer within that catchment is frozen throughout the 2-yr simulation. With few exceptions, the permafrost boundary generated by the new NSIPP scheme is highly accurate; the solid line in the figure refers to the observed permafrost line corresponding to 50% permafrost coverage whereas the dashed line corresponds to 10% permafrost coverage (Zhang et al. 1999). Similar success, however, is not found with the old Mosaic scheme, for which the southerly extent of permafrost front extends from Washington in the west to Montreal, Quebec, in the east. This comparison indicates that the three-layer model, originally developed and validated at small experimental catchments (Lynch-Stieglitz 1994; Stieglitz et al. 1999) does indeed capture the important snow processes that control the growth and the ablation of continental-scale snowpack and its snow insulation capabilities.

4. Future model developments

As stated earlier, to avoid abrupt discontinuities in the surface energy balance calculations, we account for subgrid-scale variability in snow cover when the pack is thin. However, even when snow cover is substantial, snow heterogeneity can be significant (Liston et al. 1999; Liston and Sturm 1998). Gradients in elevation; differences in aspect; and the interactions among wind, topography, and vegetation will all result in snow cover heterogeneity. In turn, this snow heterogeneity may have a profound effect on regional atmospheric dynamics via changes in the surface energy balance, and may affect the evolution of ground temperatures and the timing of the snowmelt-related discharge. We currently ignore these effects and their influence on the surface energy fluxes.

To account for elevation effects in regions of high relief, a temperature lapse rate can be used along with binned elevation bands to distribute snow cover and snowmelt throughout the landscape (Bowling and Lettenmaier 1998). To account for the effects that wind, vegetation, and topography have on the distribution of snow cover, the work of Liston and Sturm (1998) can be adapted to our modeling framework. Although their spatially explicit model is not directly compatible with the statistical treatment of topography presented here, the empirical equations governing wind-blown snow can be used to treat snow distribution in much the same way we currently treat soil moisture heterogeneity: through a statistical representation in which valleys are regions of snow accumulation and uplands are regions of snow ablation. Hartman et al. (1999) recently applied such a procedure, albeit without explicitly including for the effects of wind-blown snow, and they had success in improving snowmelt discharge.

Further improvements in the development of GCM snow schemes will increasingly rely on the use of validation datasets, especially at high latitudes. It is hoped that this effort and other ongoing efforts (Bartlett et al. 2000; Bowling and Lettenmaier 1998; Pauwels and Wood 1999; Verseghy et al. 2000), point the way toward the development of models that are computationally efficient, physically realistic, and improve seasonal-to-interannual variability in climate simulations.

5. Conclusions

General circulation model experiments predict that CO_2-induced global warming will be greatest at high northern latitudes. Associated with such rising temperatures would be increased precipitation and earlier snowmelt (Houghton et al. 1996). With this possibility in mind, researchers are attempting to answer a number of key questions: Will changes in snow cover extent and amount affect regional and global climate via changes in the surface energy balance? Will climate change augment plant growth and thus increase the uptake of CO_2 from the atmosphere? If Arctic rivers deliver less freshwater to the Arctic Ocean because of enhanced evapotranspiration, what will be the impact on river ecology, ocean shelf dynamics, surface ocean stability, and sea-ice formation? If soils become warmer, will the increased microbial activity release carbon stored in the soil? Will warmer temperatures increase the production of methane, another greenhouse gas, in regions where wetlands expand? To answer these questions on a global basis, there is a need for a new generation of computationally efficient models that can adequately represent snow processes.

We have coupled the snow model of Lynch-Stieglitz (1994) to the global catchment-based LSM of the NSIPP project. This three-layer snow model accounts for snow melting and refreezing, dynamic changes in snow density, snow insulating properties, and other physics relevant to the growth and ablation of the snowpack. Validating with 1987–88 ISLSCP datasets at over the 5000 catchments representing North America indicates that the model is capable of simulating the spatial coverage of snow. More important, the model's treatment of the insulation properties of snow cover leads to an accurate simulation of the permafrost front relative to the NSIDC digital permafrost map. Last, the successful larger-scale application of the model for North America suggests that the global application of the model is within reach and, more specifically, that application at high latitudes will be successful.

Acknowledgments. This research is a contribution to the NASA Seasonal-to-Interannual Prediction Project at Goddard Space Flight Center, supported by NASA's Global Modeling and Analysis Program under RTOP 622-24-47. This work was also supported by NSF grants from the division of Environmental Biology (Arctic LTER Project) and from the office of Polar Programs (Arctic Natural Sciences, Arctic Systems Science). Northern Hemisphere EASE-Grid Weekly Snow Cover and Sea Ice Extent data were obtained from the EOSDIS NSIDC Distributed Active Archive Center (DAAC), University of Colorado, Boulder. Jim Foster and Janet Chien at NASA GSFC provided ETAC snow climatological data. We thank T. Zhang at the Cooperative Institute for Research in Environmental Sciences at the University of Colorado for providing us with the digital permafrost map, Tim Pangburm at the Cold Regions Research and Engineering Laboratory for providing Sleepers Rivers datasets, and Doug Kane and Larry Hinzman at the University of Alaska, Fairbanks, for providing Imnavait Creek datasets.

REFERENCES

Abramopoulos, F., C. Rosenzweig, and B. Choudhury, 1988: Improved ground hydrology calculations for global climate models (GCMs): Soil water movement and evapotranspiration. *J. Climate,* **1,** 921–941.

Aguado, E., 1985: Radiation balances of melting snow covers at an open site in the central Sierra Nevada, California. *Water Resour. Res.,* **21,** 1649–1654.

Anderson, E. A., 1976: A point energy balance model of a snow cover. NOAA Tech. Rep. NWS 19, Office of Hydrology, National Weather Service, 150 pp.

Barnett, T. P., L. Dumenil, U. Schlese, E. Roeckner, and M. Latif, 1989: The effect of Eurasian snow cover on regional and global climate variations. *J. Atmos. Sci.,* **46,** 661–685.

Bartlett, P., J. H. Mccaughey, P. Lafleur, and D. L. Verseghy, 2000: Performance of the Canadian Land Surface Scheme at temperate aspen-birch and mixed forests, and a boreal young jack pine forest: Tests involving canopy conductance parametrizations. *Atmos.–Ocean,* **38,** 113–140.

Beven, K. J., and M. J. Kirkby, 1979: A physically-based variable contributing area model of basin hydrology. *Hydrol. Sci. J.,* **24,** 43–69.

Billings, W. D., J. O. Luken, D. A. Mortensen, and K. M. Peterson, 1982: Arctic tundra: A sink or source for atmospheric carbon dioxide in a changing environment. *Oecologia,* **53,** 7–11.

Bonan, G. B., 1995: Land atmosphere CO_2 exchange simulated by a land-surface process model coupled to an atmospheric general-circulation model. *J. Geophys. Res.,* **100,** 2817–2831.

——, 1996: A land surface model (LSM Version 1.0) for ecological, hydrological, and atmospheric studies: Technical description and user's guide. Tech. Note NCAR/TN-417+STR, National Center for Atmospheric Research, Boulder, CO, 150 pp.

Bowling, L. C., and D. P. Lettenmaier, 1998: A macroscale hydrological model for the Arctic basin. *Eos, Trans. Amer. Geophys. Union* (Fall Meeting Suppl.), H72D-18.

Brun, E., E. Martin, V. Simon, C. Gendre, and C. Coleou, 1989: An energy and mass model of snow cover suitable for operational avalanche forecasting. *J. Glaciol.,* **35,** 333–342.

Cohen, J., and D. Entekhabi, 1999: Eurasian snow cover variability and northern hemisphere climate predictability. *Geophys. Res. Lett.,* **26,** 345–348.

Dey, B., and O. S. R. U. Bhanukumar, 1983: Himalyan winter snow cover area and summer monsoon rainfall over India. *J. Geophys. Res.,* **88,** 5471–5474.

Dickinson, R. E., A. Henderson-Sellers, P. J. Kennedy, and M. F. Wilson, 1993: Biosphere–Atmosphere Transfer Scheme (BATS) version 1e as coupled to the NCAR Community Climate Model. Tech. Note NCAR/TN-387+STR, National Center for Atmospheric Research, Boulder, CO, 72 pp.

Ducharne, A., R. D. Koster, M. J. Suarez, M. Stieglitz, and P. Kumar, 2000: A catchment-based approach to modeling land surface processes, 2. Parameter estimation and model demonstration. *J. Geophys. Res.,* **105,** 24 823–24 838.

Famiglietti, J. S., and E. F. Wood, 1991: Evapotranspiration and runoff from large land areas—land surface hydrology for atmospheric general-circulation models. *Surv. Geophys.,* **12,** 179–204.

Foster, D. J., Jr., and R. D. Davy, 1988: Global snow depth climatology. USAF Environmental Technical Applications Center, Scott Air Force Base, IL, 43 pp.

Foster, J., and Coauthors, 1996: Snow cover and snow mass intercomparisons of general circulation models and remotely sensed datasets. *J. Climate,* **9,** 409–426.

Goulden, M. L., J. W. Munger, S. M. Fan, B. C. Daube, and S. C. Wofsy, 1996: Exchange of carbon dioxide by a deciduous forest: Response to interannual climate variability. *Science,* **271,** 1576–1578.

——, and Coauthors, 1998: Sensitivity of boreal forest carbon balance to soil thaw. *Science,* **279,** 214–217.

Hahn, D. G., and J. Shukla, 1976: An apparent relationship between the Eurasian snow cover and Indian monsoon rainfall. *J. Atmos. Sci.,* **33,** 2461–2462.

Hall, D. K., 1988: Assessment of polar climate change using satellite technology. *Rev. Geophys.,* **26,** 26–39.

Hansen, J. E., G. Russel, D. Rind, P. H. Stone, A. A. Lacis, S. Lebedeff, R. Ruedy, and L. Travis, 1983: Efficient three-dimensional global models for climate studies: Models I and II. *Mon. Wea. Rev.,* **111,** 609–662.

Hardy, J. P., R. E. Davis, R. Jordan, W. Ni, and C. E. Woodcock, 1998: Snow ablation modelling in a mature aspen stand of the boreal forest. *Hydrol. Processes,* **12,** 1763–1778.

Hartman, M. D., J. S. Baron, R. B. Lammers, D. W. Cline, L. E. Band, G. E. Liston, and C. Tague, 1999: Simulations of snow distribution and hydrology in a mountain basin. *Water Resour. Res.,* **35,** 1587–1603.

Houghton, J. T., L. G. Meira Filho, B. A. Callander, N. Harris, A. Kattenberg, and K. Maskell, Eds., 1996: *Climate Change 1995: The Science of Climate Change*. Cambridge University Press, 572 pp.

Johnson, R. H., G. S. Young, and J. J. Toth, 1984: Mesoscale weather effects of variable snow cover over northeast Colorado. *Mon. Wea. Rev.,* **112,** 1141–1152.

Jordan, R. E., E. L Andreas, and A. P. Makshtas, 1999: Heat budget of snow-covered sea ice at North Pole 4. *J. Geophys. Res.,* **104,** 7785–7806.

Kojima, K., 1967: Densification of seasonal snow cover. *Physics of Ice and Snow: Proc. Int. Conf. on Low Temperature Science,* Sapporo, Japan, Institute of Low Temperature Science, Hokkaido University, 929–952.

Koster, R. D., and M. J. Suarez, 1992a: A comparative analysis of two land surface heterogeneity representations. *J. Climate,* **5,** 1379–1390.

——, and ——, 1992b: Modeling the land surface boundary in climate models as a composite of independent vegetation stands. *J. Geophys. Res.,* **97,** 2697–2715.

——, and ——, 1995: The relative contributions of land and ocean processes to precipitation variability. *J. Geophys. Res.,* **100,** 13 775–13 790.

——, and ——, 1996: Energy and water balance calculations in the Mosaic LSM. NASA Tech. Memo. 104606, Vol. 9, 59 pp.

——, ——, A. Ducharne, M. Stieglitz, and P. Kumar, 2000a: A catchment-based approach to modeling land surface processes in a GCM. Part I: Model structure. *J. Geophys. Res.,* **105,** 24 809–24 822.

——, ——, and M. Heiser, 2000b: Variance and predictability of precipitation at seasonal-to-interannual timescales. *J. Hydrometeor.,* **1,** 26–46.

Kripalani, R. H., S. V. Singh, A. D. Vernekar, and V. Thapliyal, 1996: Empirical study on *Nimbus-7* snow mass and Indian summer monsoon rainfall. *Int. J. Climatol.,* **16,** 23–34.

Kucharik, C. J., and Coauthors, 2000: Testing the performance of a Dynamic Global Ecosystem Model: Water balance, carbon balance, and vegetation structure. *Global Biogeochem. Cycles,* **14,** 795–825.

Kumar, K. K., B. Rajagopalan, and M. A. Cane, 1999: On the weakening relationship between the Indian monsoon and ENSO. *Science,* **284,** 2156–2159.

LDEO, cited 2000: Climate data library. [Available online at http//ingrid.ldeo.columbia.edu.]

Levine, E. R., and R. G. Knox, 1997: Modeling soil temperature and snow dynamics in northern forests. *J. Geophys. Res.,* **102,** 29 407–29 416.

Liston, G. E., and M. Sturm, 1998: A snow-transport model for complex terrain. *J. Glaciol.,* **44,** 498–516.

——, R. A. Pielke, and E. M. Greene, 1999: Improving first-order snow-related deficiencies in a regional climate model. *J. Geophys. Res.,* **104,** 19 559–19 567.

Loth, B., and H. F. Graf, 1998a: Modeling the snow cover in climate studies—1. Long-term integrations under different climatic conditions using a multilayered snow-cover model. *J. Geophys. Res.,* **103,** 11 313–11 327.

——, and ——, 1998b: Modeling the snow cover in climate studies—2. The sensitivity to internal snow parameters and interface processes. *J. Geophys. Res.,* **103,** 11 329–11 340.

——, ——, and J. M. Oberhuber, 1993: Snow cover model for global climate simulations. *J. Geophys. Res.,* **98,** 10 451–10 464.

Lynch-Stieglitz, M., 1994: The development and validation of a simple snow model for the GISS GCM. *J. Climate,* **7,** 1842–1855.

McFadden, J. P., F. S. Chapin, and D. Y. Hollinger, 1998: Subgrid-scale variability in the surface energy balance of arctic tundra. *J. Geophys. Res.,* **103,** 28 947–28 961.

Mysak, L. A., and S. A. Venegas, 1998: Decadal climate oscillations in the Arctic: A new feedback loop for atmosphere–ice–ocean interactions. *Geophys. Res. Lett.,* **25,** 3607–3610.

Namias, J., 1985: Some empirical evidence for the influence of snow cover on temperature and precipitation. *Mon. Wea. Rev.,* **113,** 1542–1553.

NSIDC, 1996: Northern Hemisphere EASE-Grid weekly snow cover and sea ice extent. Volumes 1.0–2.0, National Snow and Ice Data Center, CD-ROM.

Oechel, W. C., G. Vourlitis, and S. J. Hastings, 1997: Cold season CO_2 emission from arctic soils. *Global Biogeochem. Cycles,* **11,** 163–172.

Pauwels, V. R. N., and E. F. Wood, 1999: A soil–vegetation–atmosphere transfer scheme for the modeling of water and energy balance processes in high latitudes. 2. Application and validation. *J. Geophys. Res.,* **104,** 27 823–27 839.

Pitman, A. J., Z.-L. Yang, J. G. Cogley, and A. Henderson-Sellers, 1991: Description of bare essentials of surface transfer for the Bureau of Meteorological Research Centre AGCM. BMRC Research Rep. 32, 132 pp.

Ropelewski, C. F., A. Robock, and M. Matson, 1984: Comments on ''An apparent relationship between the Eurasian snow cover and Indian monsoon rainfall.'' *J. Climate Appl. Meteor.,* **23,** 341–342.

Segal, M., J. H. Cramer, R. A. Pielke, J. R. Garratt, and P. Hildebrand, 1991: Observational evaluation of the snow breeze. *Mon. Wea. Rev.,* **119,** 412–424.

Sellers, P. J., Y. Mintz, Y. C. Sud, and A. Dalcher, 1986: A Simple Biosphere Model (Sib) for use within general circulation models. *J. Atmos. Sci.,* **43,** 505–531.

——, and Coauthors, 1996: The ISLSCP Initiative I global datasets: Surface boundary conditions and atmospheric forcings for land–atmosphere studies. *Bull. Amer. Meteor. Soc.,* **77,** 1987–2005.

Sivapalan, M., K. Beven, and E. F. Wood, 1987: On hydrologic similarity. 2. A scaled model of storm runoff production. *Water Resour. Res.,* **23,** 2266–2278.

Slater, A. G., A. J. Pitman, and C. E. Desborough, 1998: The validation of a snow parameterization designed for use in general circulation models. *Int. J. Climatol.,* **18,** 595–617.

Stieglitz, M., D. Rind, J. Famiglietti, and C. Rosenzweig, 1997: An efficient approach to modeling the topographic control of surface hydrology for regional and global climate modeling. *J. Climate,* **10,** 118–137.

——, J. Hobbie, A. Giblin, and G. Kling, 1999: Hydrologic modeling of an arctic tundra watershed: Toward pan-Arctic predictions. *J. Geophys. Res.,* **104,** 27 507–27 518.

——, A. Giblin, J. Hobbie, G. Kling, and M. Williams, 2000: Simulating the effects of climate change and climate variability on carbon dynamics in Arctic tundra. *Global Biogeochem. Cycles,* **14,** 1123–1136.

Verdin, K. L., and J. P. Verdin, 1999: A topological system for delineation and codification of the earth's river basins. *J. Hydrol.,* **218,** 1–12.

Verseghy, D. L., 1991: CLASS—a Canadian Land Surface Scheme for GCMS. 1. Soil model. *Int. J. Climatol.,* **11,** 111–133.

——, I. R. Saunders, J. D. Bowers, Z. Huo, and W. G. Bailey, 2000: Application of the Canadian Land Surface Scheme to the simulation of energy and water fluxes over Alpine tundra. *Atmos.–Ocean,* **38,** 37–55.

Walter, B. P., M. Heimann, R. D. Shannon, and J. R. White, 1996: A process-based model to derive methane emissions from natural wetlands. *Geophys. Res. Lett.,* **23,** 3731–3734.

Wood, E. F., and Coauthors, 1998: The Project for Intercomparison of Land-Surface Parameterization Schemes (PILPS) phase 2(c) Red–Arkansas River Basin experiment: 1. Experiment description and summary intercomparisons. *Global Planet. Change,* **19,** 115–135.

Yang, Z. L., R. E. Dickinson, A. Robock, and K. Y. Vinnikov, 1997: Validation of the snow submodel of the Biosphere–Atmosphere Transfer Scheme with Russian snow cover and meteorological observational data. *J. Climate,* **10,** 353–373.

Zhang, T., R. G. Barry, and K. Knowles, 1999: Statistics and characteristics of permafrost and ground ice distribution in the Northern Hemisphere. *Polar Geogr.,* **22,** 147–169.

Zimov, S. A., I. P. Semiletov, S. P. Daviodov, Y. V. Voropaev, S. F. Prosyannikov, C. S. Wong, and Y. H. Chan, 1993: Wintertime CO_2 emission from soils of northeastern Siberia. *Arctic,* **46,** 197–204.

——, S. P. Davidov, Y. V. Voropaev, S. F. Prosiannikov, I. P. Semiletov, M. C. Chapin, and F. S. Chapin, 1996: Siberian CO_2 efflux in winter as a CO_2 source and cause of seasonality in atmospheric $C0_2$. *Climatic Change,* **33,** 111–120.